High-Mobility Air-Stable Naphthalene Diimide-Based Copolymer Containing Extended π-Conjugation for n-Channel Organic Field Effect Transistors

Ran Kim, Paul S. K. Amegadze, Il Kang, Hui-Jun Yun, Yong-Young Noh, Soon-Ki Kwon,* and Yun-Hi Kim**

A high-performance naphthalene diimide (NDI)-based conjugated polymer for use as the active layer of n-channel organic field-effect transistors (OFETs) is reported. The solution-processable n-channel polymer is systematically designed and synthesized with an alternating structure of long alkyl substituted-NDI and thienylene–vinylene–thienylene units (PNDI-TVT). The material has a well-controlled molecular structure with an extended π-conjugated backbone, with no increase in the LUMO level, achieving a high mobility and highly ambient stable n-type OFET. The top-gate, bottom-contact device shows remarkably high electron charge-carrier mobility of up to 1.8 $cm^2 V^{-1} s^{-1}$ ($I_{on}/I_{off} = 10^6$) with the commonly used polymer dielectric, poly(methyl methacrylate) (PMMA). Moreover, PNDI-TVT OFETs exhibit excellent air and operation stability. Such high device performance is attributed to improved π–π intermolecular interactions owing to the extended π-conjugation, apart from the improved crystallinity and highly interdigitated lamellar structure caused by the extended π–π backbone and long alkyl groups.

1. Introduction

Solution-processable conjugated polymers have been intensively studied for use in organic field effect transistors (OFETs) because they can be employed in various flexible and large-area electronic applications through cost-effective printing techniques.[1–7] Recently, various p-channel polymers with impressively high hole mobility have been successfully developed.[8] However, only limited progress has been made in producing n-channel conjugated polymers for use as active layers in OFETs owing to the difficult chemistry involved in the synthesis of materials with high stability in air. Semiconductors with n-channel conjugated polymers need to be able to form complementary integrated circuits (ICs) with p-channel materials, which exhibit lower power consumption and larger noise margin than unipolar ICs.[9] The major trap sites for electrons in the band gap are mainly located at 3.8–4.0 eV because of hydrogenated oxygen, that is, humid air.[10] This means that n-channel semiconductors must have a lower lowest unoccupied molecular orbital (LUMO) level than that of the trap sites; deeper LUMO levels provide better ambient stability for n-channel OFETs. However, it is very difficult to synthesize conjugated polymers with such low-lying LUMO levels because most commonly used building blocks are rich in electrons.

Among the rare building blocks useful for producing n-channel polymers, rylene diimides, especially perylene and naphthalene derivatives, have so far proved to be the most successful air-stable electron-transporting (n-type) units.[11–15] The electron-accepting naphthalene diimide (NDI) unit provides a planar conjugated bicyclic structure, which leads to strong π–π interactions that provide better charge-transporting properties between chains. In addition, the introduction of alkyl chains at the N-position of the imide ring affords control over physical properties such as solubility, crystallization, and self-assembly capability. Moreover, the presence of two strong electron-withdrawing diimide groups for each naphthalene moiety pulls down the LUMO level, thus increasing the air stability of the n-type semiconductor. NDI polymers are now attracting increasing attention, particularly after a recent report concerning a soluble NDI–bithienyl copolymer that was capable of being used in printable electronics applications. This was reported to achieve OFET electron mobility of up to 0.85 $cm^2 V^{-1} s^{-1}$ using top-gate bottom-contact device architectures with polymeric dielectrics.[15–17] Despite the highly improved electron mobility and ambient stabilities of recently reported NDI polymer-based OFETs, enhanced characteristics are needed to meet the requirements of commercial applications and provide a performance balance with state-of-the-art p-channel conjugated polymers.[18]

R. Kim, Prof. Y.-H. Kim
Department of Chemistry and RINS
Gyeongsang National University
501 Jinju Daero, Jinju, 660-701, Republic of Korea
E-mail: ykim@gnu.ac.kr

P. S. K. Amegadze, Prof. Y.-Y. Noh
Department of Energy and Materials Engineering
Dongguk University
26, Pil-dong, 3-ga, Jung-gu, Seoul, 100-715, Republic of Korea
E-mail: yynoh@dongguk.edu

I. Kang, H.-J. Yun, Prof. S.-K. Kwon
School of Materials Science & Engineering and ERI
Gyeongsang National University
501 Jinju Daero, Jinju, 660-701, Republic of Korea
E-mail:skwon@gnu.ac.kr

DOI: 10.1002/adfm.201301197

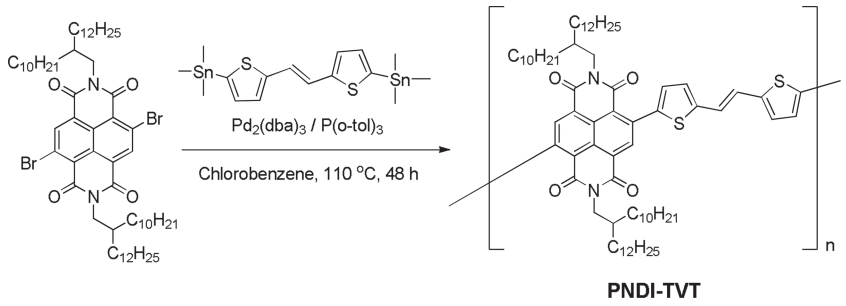

Scheme 1. Synthesis of PNDI-TVT.

Here, we report the preparation of a solution-processed polymer, poly[(*E*)-2,7-bis(2-decyltetradecyl)-4-methyl-9-(5-(2-(5-methylthiophen-2-yl)vinyl)thiophen-2-yl)benzo[lmn][3,8] phenanthroline-1,3,6,8(2*H*,7*H*)-tetraone] (PNDI-TVT), the molecular structure of which is shown in **Scheme 1**. To achieve n-type FETs with high mobility and ambient stability, PNDI-TVT was designed with an alternating structure consisting of NDI and thienylene–vinylene–thienylene (TVT) units, which have a vinyl linkage between adjacent thiophene units. Incorporating this group would extend the conjugation length and improve the molecular rigidity, thereby preventing the adjacent thiophene rings from rotating.[19–21] This, in turn, would increase the degree of coplanarity of the polymer backbone, which should drive the assembly of the polymer chains. In addition, the strong donor–acceptor interaction could enhance intermolecular interactions because the polymer has an alternating structure comprising NDI as an electron acceptor unit and TVT as a donor unit. Therefore, the polymer would have large intermolecular overlap through the π–π stacking that arises from the rigid and extended coplanar conjugated polymer backbone and donor–acceptor interaction. This would reduce the distance between the polymer chains in the thin-film state and enforce long-range ordering of the molecules, allowing more crystalline structures.

Furthermore, the extended π-conjugation would affect the highest occupied molecular orbital (HOMO) level but not the LUMO, which could improve its air stability. The introduction of long bis(2-decyltetradecyl) alkyl chains should enhance the solubility of the rigid molecular structure, as well as better air stability through self-passivation. Therefore, here, we report that the PNDI-TVT material exhibited an n-type field effect mobility value as high as 1.8 $cm^2\ V^{-1}\ s^{-1}$ (average: 1.5 $cm^2\ V^{-1}\ s^{-1}$) and excellent air and operation stabilities. To the best of our knowledge, this is the highest n-type mobility that has been achieved by n-channel conjugated polymers.

2. Results and Discussion

Scheme 1 shows the structures of the monomer and PNDI-TVT copolymer, along with the conditions for the polymerization reaction. PNDI-TVT was prepared using a Pd-catalyzed Stille coupling reaction between (E)-1,2-bis(5-(trimethylstannyl) thiophene-2-yl)ethene and 4,9-dibromo-2,7-bis(2-decyltetradecyl)benzo[lmn][3,8]phenanthroline-1,3,6,8(2*H*,7*H*)-tetraone. After the polymer was purified using successive Soxhlet extraction with acetone, methanol, and hexane to remove the metal catalyst, it was dissolved in chloroform and then precipitated using methanol. The structure of the polymer was confirmed by ^{1}H NMR (Supporting Information, Figure S1). The polymer had good solubility in common organic solvents such as toluene, chloroform, chlorobenzene, and 1,2-dichlorobenzene, despite its rigid planar structure. This may be because of the long branched bis(2-decyltetradecyl) alkyl chains.

The number average molecular weight (M_n) of PNDI-TVT was determined using gel permeation chromatography (GPC) analysis against polystyrene standards and was found to be 70 000 g mol^{-1} with a polydispersity index (PDI) (M_w/M_n) of 1.98.

PNDI-TVT was found to exhibit very good thermal stability, with 5% weight loss at 453 °C, as determined by thermogravimetric analysis (TGA) under a N_2 atmosphere. The thermal transition properties of the polymer were investigated using differential scanning calorimetry (DSC). A discrete endothermic peak was visible on heating at 230 °C, and an exothermic peak on cooling at 210 °C, indicating that PNDI-TVT had crystallinity (**Figure 1**).

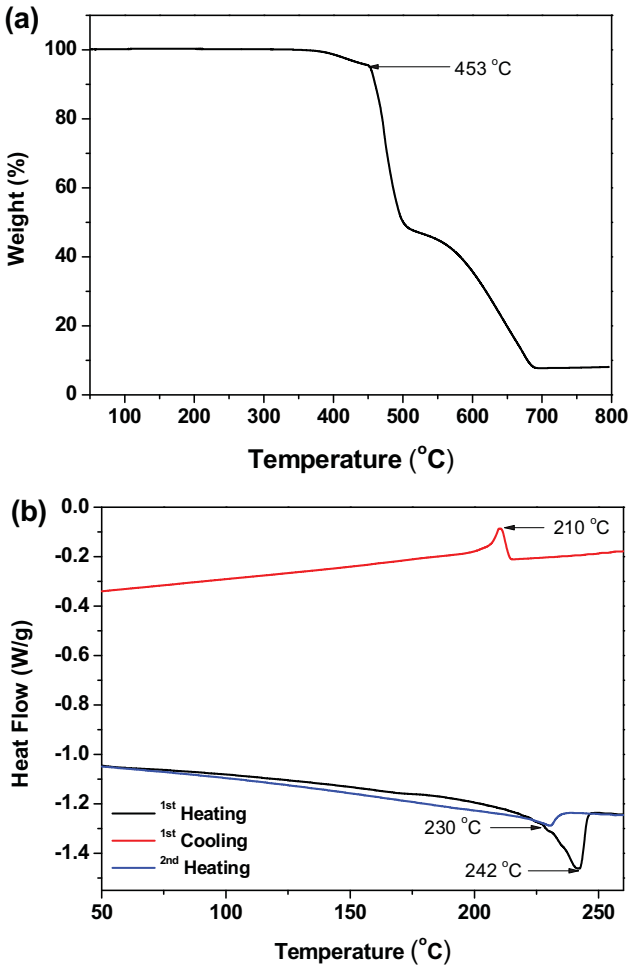

Figure 1. a) TGA thermogram and b) DSC thermogram of PNDI-TVT in a N_2 atmosphere at a scan rate of 10 °C min^{-1}.

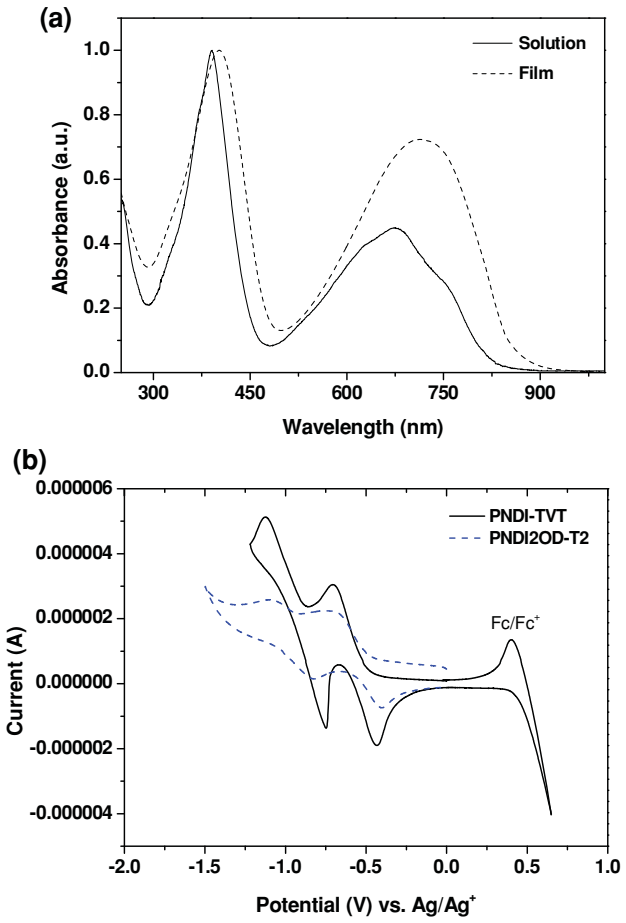

Figure 2. a) UV-vis spectra of PNDI-TVT in $CHCl_3$ solution and as a thin film. b) Cyclic voltammograms of PNDI-TVT and PNDI2OD-T2.

Optical absorption spectra of PNDI-TVT in dilute (10^{-6} M) chloroform solution and solid film state are shown in **Figure 2**a. Two distinct absorption bands can be seen in the solution spectrum, which were assigned as a π–π^* transition at 390 nm and an intramolecular charge transfer (ICT) band at 675 nm caused by its donor–acceptor structure. The corresponding absorption peaks in the thin film can be observed at 403 nm and 716 nm. The ICT band in the spectrum of the film state showed a significant red-shift and was broadened. This is presumably because of the occurrence of well-ordered intermolecular interactions between the rigid and coplanar polymer molecules in the solid state. The optical band gap of PNDI-TVT was found to be 1.42 eV, calculated from the onset absorption (λ_{max} = 872 nm) of the thin film. When the results were compared with those reported for the bithiophene-containing polymer, PNDI2OD-T2, the π–π^* transition and ICT band of PNDI-TVT were 10- and 20-nm red-shifted, respectively.[22] In addition, the optical band gap was narrower. These results can be explained by the presence of an extended π-conjugation because of the introduction of the vinyl group in the TVT unit, leading to more effective intermolecular interactions.

To estimate the positions and energies of the frontier orbitals for NDI-TVT and PNDI2OD-T2, density functional theory (DFT) calculations were performed at the B3LYP 6-31G** level. N-alkyl chains were replaced by an N-methyl group and repeating units (NDI and TVT for NDI-TVT; NDI and bithiophene for PNDI2OD-T2) were used in the calculations. As shown in **Figure 3**, the coefficients of the HOMO orbital are located on the TVT moiety, while those of the LUMO orbital are mainly positioned on the central NDI unit. The calculated energy gap of PNDI-TVT was narrower than that of PNDI2OD-T2, consistent with the optical band gap results. Interestingly, the introduction of TVT in place of bithiophene led to a reduced band gap and increased HOMO energy level, but did

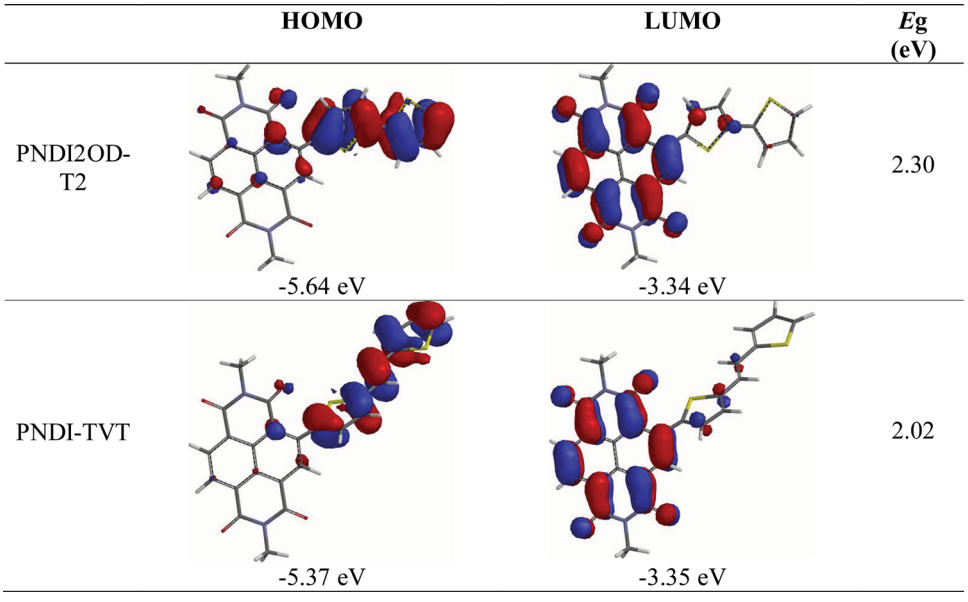

Figure 3. Calculated stereostructures and frontier orbitals of PNDI2OD-T2 and PNDI-TVT.

Table 1. Physical properties of PNDI-TVT.

Polymer	Yield [%]	M_n [kDa]	λ_{abs} [nm]		T_d [°C]	LUMO [eV][a)]	HOMO [eV][b)]	E_g [eV]
			Solution	Film				
PNDI-TVT	91	70	390, 675	403, 716	453	−4.00	−5.42	1.42

[a)] $E_{LUMO} = -(E_{1/2}^{red-1} + 4.43\ eV)$; [b)] $E_{HOMO} = E_{LUMO} - E_g$ (estimated from optical absorption spectrum).

not change the LUMO energy level. These results suggest that the electron density of HOMO is controlled by the donor unit, while that of LUMO is controlled by the acceptor NDI unit. The calculation results show that PNDI-TVT and PNDI2OD-T2 have similar dihedral angles. The angles between the NDI and TVT units were 33.44° and 32.82°, respectively, when calculated using two repeating units of NDI and TVT, while those between NDI and bithiophene units were 32.88° and 40.61°, respectively (Supporting Information, Figure S2). The similar dihedral angle may be due to a much larger size of NDI unit than TVT or bi-thiophene unit, even though the better coplanarity is expected due to the rigid TVT unit.

The electrochemical behavior of the PNDI-TVT film was measured by using cyclic voltammetry (CV) to determine its ionization potential. The voltammogram of PNDI-TVT shows two reversible reductions, with first and second half-wave potentials at −0.43 and −0.75 V, respectively, while those of PNDI2OD-T2 can be seen at −0.40 and −0.82 V under the same conditions (Figure 2b). The corresponding LUMO energy of PNDI-TVT and PNDI2OD-T2 was approximately −4.0 eV (**Table 1**). The reported LUMO-energy-stability correlations showed that the LUMO energy of PNDI-TVT is adequate for thin-film transistor (TFT) ambient operation without diminishing the air stability.[22]

The high electron mobility and air stability of PNDI-TVT can be understood by its solid-state morphology, molecular packing, and crystallinity, which were investigated by X-ray diffraction (XRD) and atomic force microscopy (AFM). As show in **Figure 4**, the XRD pattern of the polymer thin film contains a weak diffraction peak at $2\theta = 3.2°$, corresponding to a d-spacing of 27.59 Å. After thermal annealing at 150–210 °C, the diffraction intensity increased, with first-, second-, and third-order peaks (at 3.7°, 6.8°, and 9.11°, respectively) appearing, indicating the presence of a highly ordered lamellar structure perpendicular to the substrate. Furthermore, the long alkyl chains of PNDI-TVT show enhanced intermolecular side-chain ordering such as interdigitation or end-to-end packing upon thermal annealing ($2\theta = 3.7°$, 23.86 Å). The XRD results demonstrate increases in both the edge-on orientation peak at $2\theta = 3.2°$ and the face-on orientation peak at $2\theta = 20°–30°$. The results indicate that the film consists of a mixed structure of face-on and edge-on oriented molecules. Such morphology would be expected to give better charge-carrier mobility as well as better ambient stability for OFETS employing the NDI-TVT polymer compared to the PNDI2OD-T2. Fabiano et al. recently reported that the mixed morphology PNDI2OD-T2 film had enhanced charge-carrier mobility compared to the 100% edge-on configuration, where the hydrophobic side chains acted as insulators and did not allow charge percolation in the vertical direction through the semiconducting layer.[23] In addition, some amount of edge-on orientation provides better ambient stability than 100% face-on orientation, that is, in the PNDI2OD-T2 film, because of the encapsulation effect of the vertically aligned long alkyl side chains. In the AFM images of pristine and annealed NDI-TVT films shown in **Figure 5**, large connected grains with a terrace-like step structure can be observed after thermal annealing at 150–210 °C, which also indicates a highly ordered lamellar structure. Even though this lamellar morphology was observed, the annealed film surface demonstrated greater roughness than a film surface consisting of 100% edge-on molecular orientation, indicating a mixture of face-on and edge-on orientations. It is well known that polymers with interdigitated structures exhibit better electrical performance, as well as superior

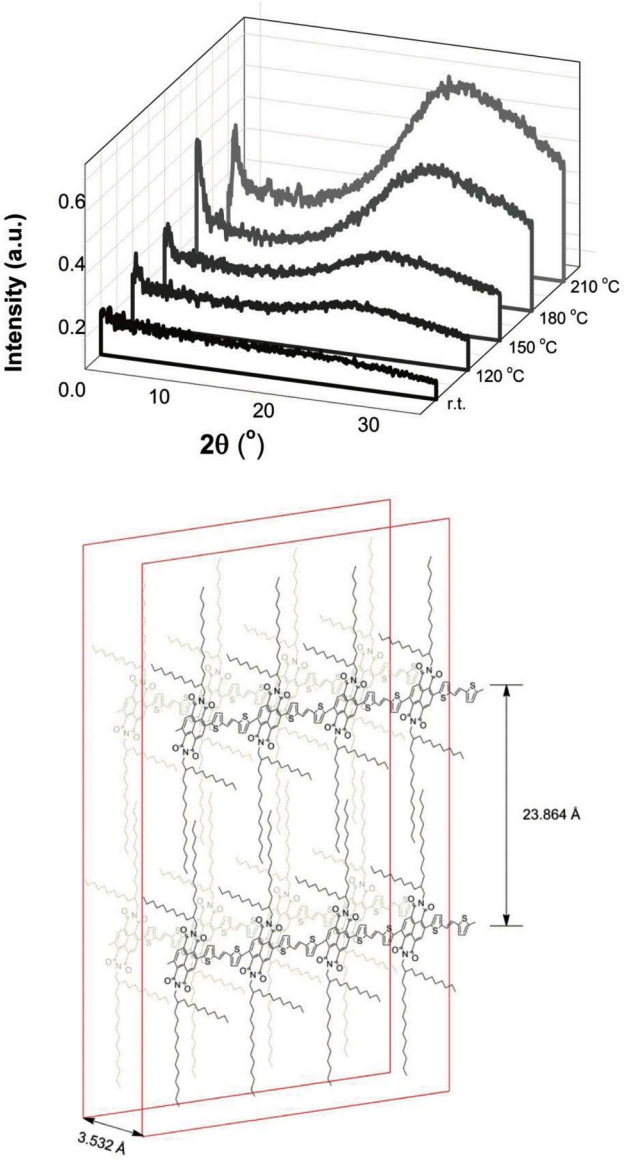

Figure 4. XRD patterns of PNDI-TVT.

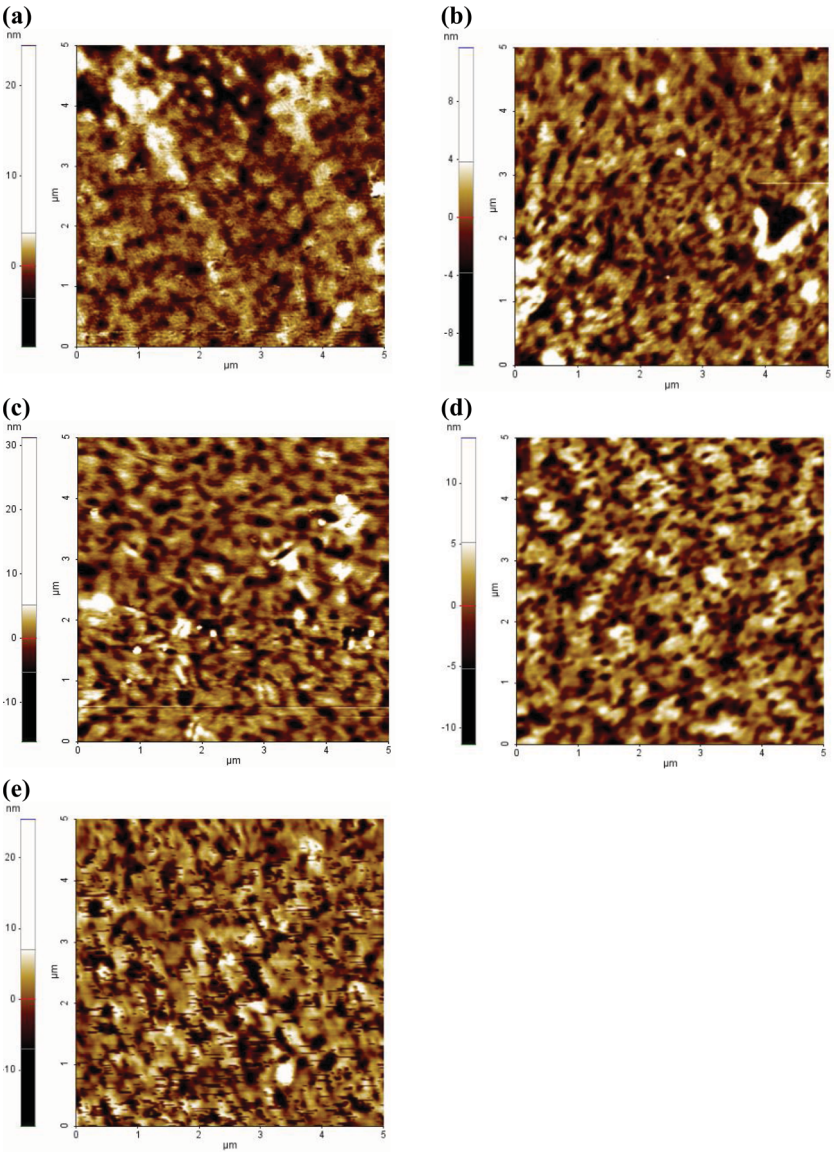

Figure 5. AFM images of PNDI-TVT: a) pristine, b) after annealing at 120 °C, c) after annealing at 150 °C, d) after annealing at 180 °C, and e) after annealing at 210 °C.

stability to O_2 and H_2O.[24,25] The crystallinity of PNDI-TVT could be comparable with that of PNDI2OD-T2, which exhibits negligible Bragg reflection intensities under all film thermal annealing conditions.[17] The better crystallinity and the mixed thin-film morphology of PNDI-TVT should provide increased air stability as well as high electron mobility.

Figure 6a,b show the transfer characteristics of top-gate and bottom-contact PNDI-TVT OFETs with bare and Cs_2CO_3-treated Au source (S) and drain (D) electrodes. The OFETs were fabricated using fresh PNDI-TVT films or those annealed at temperatures varying from 120 to 210 °C. Both the electron and hole mobility were highly improved by the thermal annealing process. Electron (and hole) mobility progressively increased from 0.15 (0.016) for pristine to 1.4 (0.14) $cm^2\ V^{-1}\ s^{-1}$ for devices with a bare Au S/D electrode annealed at 150–210 °C. These results are consistent with the film crystallinity and morphology observed by XRD and AFM. The electron mobility of the newly developed PNDI-TVT copolymer described in this study is the highest among the reported solution-processable NDI-based polymeric semiconductors. It is almost twice that of reported for PNDI2OD-T2. The most effective device exhibited an electron mobility of 1.8 $cm^2\ V^{-1}\ s^{-1}$, with a Cs_2CO_3-treated Au electrode, after annealing at 150–210 °C. **Table 2** summarizes the basic characteristics of the PNDI-TVT OFETs. Interestingly, similar high electron mobility (≈1.2 $cm^2\ V^{-1}\ s^{-1}$) was achieved for non-annealed PNDI-TVT OFETs by inserting a thin Cs_2CO_3 interlayer (≈1 nm) between the semiconductor and the Au electrode. This indicates that the main reason for low electron mobility in the pristine device (without annealing and Cs_2CO_3) was inefficient electron injection from the high work-function Au to the LUMO energy level of PNDI-TVT. Moreover, the results from the Cs_2CO_3-based devices indicate that thermal annealing significantly improved the electron-injection properties by slightly increasing the crystallinity of the PNDI-TVT film.[26] The p-channel characteristics in the originally ambipolar PNDI-TVT OFETs completely disappeared with the insertion of Cs_2CO_3 because of its hole-blocking property.[27]

One major issue for n-channel conjugated polymers is the poor ambient and bias stress stability, which mainly results from trap sites owing to hydrated O_2.[10] Compared with p-channel conjugated polymers, the electrical properties of n-channel polymers are easily degraded in ambient conditions by the generation of deep trap sites in the band gap caused by O_2 and H_2O.[18] Therefore, the ambient and bias stabilities of PNDI-TVT OFETs were evaluated by monitoring the electrical characteristics of the device with respect to storage time in air and continuous operation. State-of-the-art high-performance n-type PNDI2OD-T2 OFETs were used as reference devices owing to their known excellent air stability.[17] Both PNDI2OD-T2 and PNDI-TVT films were annealed on a 120 °C hot plate for 20 min. As shown in **Figure 7**, the electrical characteristics of PNDI-TVT OFETs were almost unchanged after four days of storage in air, while the drain current of PNDI2OD-T2 OFETs slightly decreased (**Figure 8**). After five days, the drain current of PNDI-TVT OFET remained similar or slightly increased, while that of the PNDI2OD-T2 device marginally decreased (Figures 7a,8). This indicates that a smaller number of trap sites were generated in the PNDI-TVT film using O_2 and H_2O in the air atmosphere compared to the PNDI2OD-T2 film. The presence of defects at the semiconductor–insulator interface and in the semiconductor layer can result in the degradation of the device under continuous operating conditions;

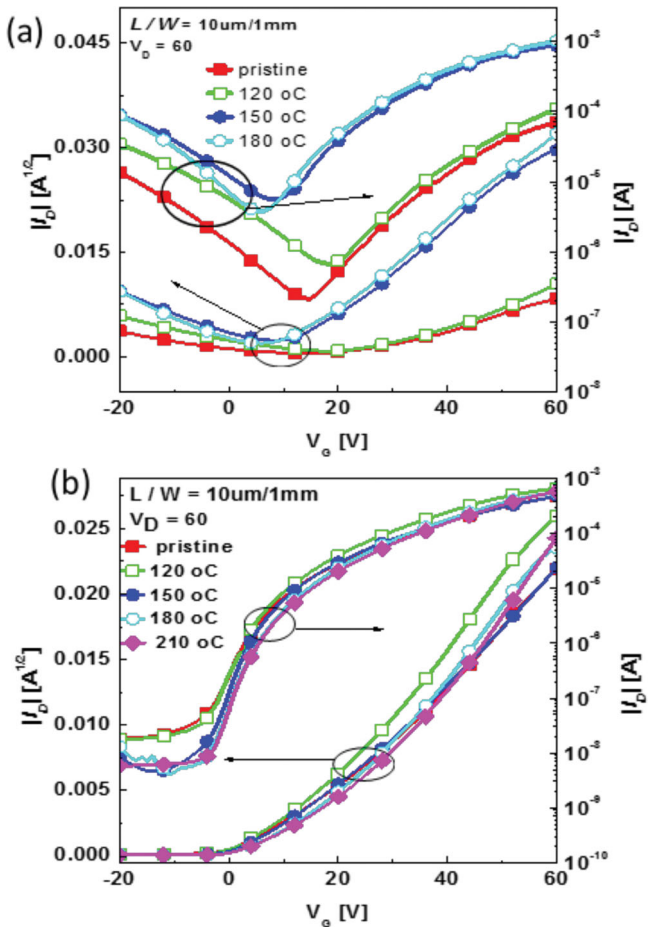

Figure 6. Transfer characteristics of PNDI-TVT OFETs with a) Au or b) Cs_2CO_3 on Au source/drain electrodes. OFETs were fabricated with pristine or annealed PNDI-TVT film annealed at a temperature of 120, 150, 180, and 210 °C. c) Dotted lines indicate gate-source current (I_g) to check gate-leakage current.

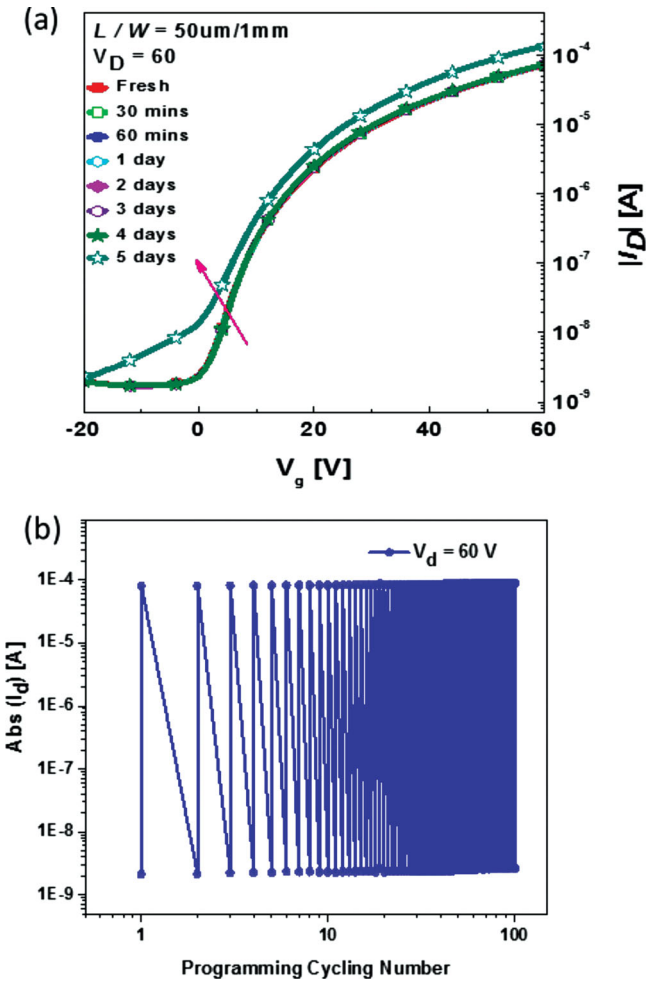

Figure 7. a) Transfer characteristics in the saturation region of PNDI-TVT OFETs as a function of time. Devices were kept in the dark and exposed to air with humidity of 25–30%. b) Cycling voltage test of PNDI-TVT OFETs at V_d = 60 V, V_g = 60 or 0 V.

however, the devices that were stored for five days showed similar electron mobility (1.3–1.5 $cm^2\ V^{-1}\ s^{-1}$) and other characteristics compared to freshly prepared devices. Other transistor parameters for the ambient stability tests are summarized in **Table 3**. Figure 7b shows the on and off currents of PNDI-TVT OFETs at V_D = 60 V for 100 cycling scans in ambient conditions. The on and off currents of PNDI-TVT OFETs were on average 2.52×10^{-9} A (V_g = 0 V) and 8.61×10^{-5} A (V_g = 60 V) throughout the scan period. These results indicate that PNDI-TVT OFETs had significantly high stability in ambient conditions and under

Table 2. Fundamental parameters of PNDI-TVT OFET devices with various annealing temperatures: electrode, W/L = 1 mm/10–50 μm).

Semiconductor/ Dielectrics	Annealing Temperature [°C]	S/D electrode	At V_d = 60 V V_g = 60 V			At V_d = −60 V V_g = −60 V		
			$\mu_{e,FET}$ [$cm^2\ V^{-1}s^{-1}$]	$V_{e,Th}$ [V]	I_{on}/I_{off}	$\mu_{h,FET}$ [$cm^2\ V^{-1}\ s^{-1}$]	$V_{h,Th}$ [V]	I_{on}/I_{off}
PNDI-TVT/PMMA	Pristine	Au	0.15 (±0.02)	24.31	~10^3	0.016 (±0.001)	−65	~10^2
		Cs_2CO_3/Au	1.20 (±0.2)	12.49	~10^4	NA	NA	NA
	120	Au	0.6 (±0.1)	26.13	~10^3	0.11 (±0.01)	−68	~10^2
		Cs_2CO_3/Au	1.20 (±0.15)	12.60	~10^5	NA	NA	NA
	150	Au	1.4 (±0.25)	9.89	~10^3	0.14 (±0.02)	−72	~10^1
		Cs_2CO_3/Au	1.5 (±0.3)	12.60	~10^6	NA	NA	NA
	180	Au	1.4 (±0.2)	7.33	~10^3	0.14 (±0.02)	−70	~10^1
		Cs_2CO_3/Au	1.5 (±0.3)	13.07	~10^6	NA	NA	NA
	210	Cs_2CO_3/Au	1.5 (±0.2)	17.7	~10^6			

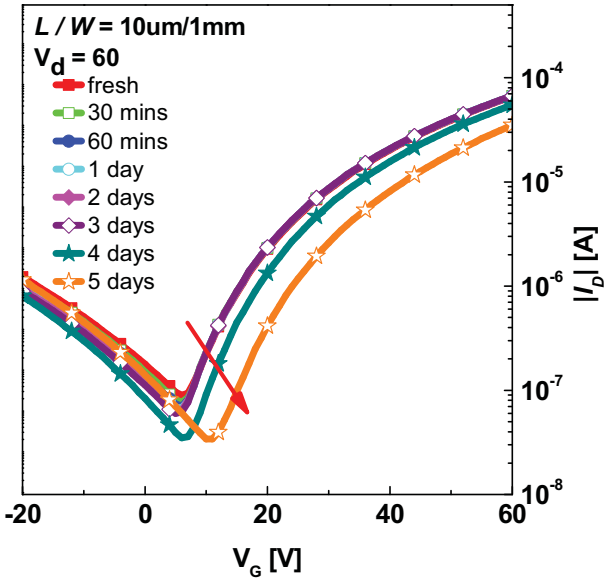

Figure 8. Transfer characteristics in the saturation region of PNDI2OD-T2 OFETs as a function of time.

continuous bias stress. The presence of the auto-encapsulation effect of the overlaid gate and gate dielectric layer would provide ambient stability for the top-gated PNDI-TVT FETs; however, the reference PNDI2OD-T2 OFETs were fabricated with the same top-gated configuration but showed inferior characteristics. Therefore, it was concluded that the new NDI-based polymer had better ambient and stress stability than PNDI2OD-T2. The higher ambient stability of PNDI-TVT FETs is mainly because of the morphology of the polymer film, with its mixture of edge-on and face-on orientation, auto-encapsulation effect by the overlaid gate and gate dielectric layer, and low LUMO energy level of the specifically designed polymer.

3. Conclusions

We designed and synthesized a new solution-processable n-channel polymer with an extended π-conjugated backbone, without increasing the LUMO level. The obtained polymer, PNDI-TVT, had a well-controlled alternating structure consisting of a long alkyl chain-substituted NDI as an electron acceptor unit and TVT as a donor unit. The PNDI-TVT copolymer demonstrated a remarkably high electron-carrier mobility of up to 1.8 $cm^2\ V^{-1}\ s^{-1}$ ($I_{on}/I_{off} = 10^6$) and high air and bias stress stability. To the best of our knowledge, this newly developed material showed the highest n-type mobility, in combination with excellent air and operation stabilities, among the reported n-channel conjugated polymers. The superior performance of PNDI-TVT OFET was attributed to improved π–π intermolecular interactions because of the extended π-conjugation, improved crystallinity with a highly interdigitated lamellar structure owing to the extended backbone and long alkyl groups, and mixed face-on and edge-on orientation.

4. Experimental Section

Materials and Characterization: All starting materials were purchased from Aldrich, TCI, and Alfa, and were used without further purification.

^{1}H NMR spectra were recorded using a Bruker Avance 300 MHz and Bruker 500 FT-NMR spectrometer; chemical shifts (ppm) were reported

Table 3. Summary of the electrical characteristics of PNDI-TVT and PNDI2OD-T2 OFETs that were kept in the dark and exposed to air with a humidity of 25–30%.

Semiconductor/Dielectrics	Time	At $V_d = 60$ V, $V_g = 60$ V, $L_{channel} = 50$ µm		
		$\mu_{e,FET}$ [$cm^2\ V^{-1}\ s^{-1}$]	$V_{e,Th}$ [V]	I_{on}/I_{off}
PNDI-TVT/PMMA	fresh	0.65 ±0.15	17.7	~10^5
	30 min	0.64 ± 0.06	17.2	~10^5
	60 min	0.64 ± 0.04	17.2	~10^5
	1 day	0.64 ± 0.05	17.2	~10^5
	2 days	0.62 ± 0.08	16.5	~10^5
	3 days	0.62 ± 0.01	16.5	~10^5
	4 days	0.61 ± 0.02	16.1	~10^5
	5 days	0.6 ± 0.10	18.0	~10^5
P(NDI2OD-T2)/PMMA	fresh	0.25 ± 0.021	18.5	~10^3
	30 min	0.25 ± 0.014	18.4	~10^3
	60 min	0.25 ± 0.018	18.8	~10^3
	1 day	0.26 ± 0.15	17.8	~10^3
	2 days	0.25 ± 0.02	18.1	~10^3
	3 days	0.26 ± 0.06	19.0	~10^3
	4 days	0.24 ± 0.04	21.3	~10^3
	5 days	0.21 ± 0.10	27.0	~10^3

with tetramethylsilane as an internal standard. Fourier transform (FT)-IR spectra were recorded using a Bruker IFS66 spectrometer. TGA was performed under N_2 using a TA instrument 2050 TG analyser. DSC was conducted under N_2 using a TA instrument DSC Q10, and both samples were heated at a rate of 10 °C min^{-1}. UV-vis spectra were measured using a Shimadsu UV-1065PC UV-vis spectrophotometer. The electrochemical properties of the materials were measured by CV using Epsilon C3 in 0.1 M solution of tetrabutyl ammonium perchlorate in chloroform. Molecular weights and polydispersities of the copolymers were determined by GPC analysis with polystyrene standard calibration (Waters high-pressure GPC assembly Model M515 pump, u-Styragel columns of HR4, HR4E, HR5E, with 500 and 100 Å, refractive index detectors, solvent: THF).

*Synthesis of 4,9-dibromoisochromeno[6,5,4-def]isochromene-1,3,6,8-tetraone (NDA-Br_2) (**1**)*: A mixture of 1,4,5,8-naphthalenetetracarboxylic dianhydride (17.60 g, 65.64 mmol) and oleum (20% SO_3, 100 mL) was stirred at room temperature for 1 h. A solution of dibromoisocyanuric acid (18.83 g, 65.64 mmol) in oleum (50 mL) was stirred at room temperature for 1 h. The dibromoisocyanuric acid solution was then poured into the 1,4,5,8-naphthalenetetracarboxylic dianhydride, and the resulting mixture was warmed to 40 °C and maintained at this temperature for 5 h. After cooling to room temperature, the reaction mixture was poured onto crushed ice (500 g), followed by the addition of H_2O (1000 mL), and then stirred at room temperature for 1 h. The precipitates were collected by centrifugation, washed with H_2O and methanol, and dried under vacuum, leading to a greenish-yellow solid. This material was used for the next step without further purification. Yield: 94% (26.28 g). ^{1}H NMR (300 MHz, $CDCl_3$, δ): 8.71 (s, 2H); IR (KBr, cm^{-1}): ν = 1786, 1746.

*Synthesis of 4,9-dibromo-2,7-bis(2-decyltetradecyl)benzo[lmn][3,8]phenanthroline-1,3,6,8(2H,7H)-tetraone (NDI-Br_2) (**2**)*: NDA-Br_2 (**1**) (10.00 g, 23.47 mmol) was added to a 500 mL round bottom flask along with glacial acetic acid (200 mL) and 2-decyltetradecan-1-amine (20.75 g, 58.68 mmol). The reaction mixture was refluxed under N_2 for 1 h and then poured onto H_2O, forming a precipitate that was subsequently filtered and washed with methanol. The crude product was purified via column chromatography over silica gel (eluent: dichloromethane/hexane, 1:1). NDI-Br_2 (**2**) was obtained as an orange-pink solid. Yield: 40% (10.36 g). ^{1}H NMR (300 MHz, $CDCl_3$, δ): 9.01 (s, 2H), 4.16–4.14 (t, 4H), 2.15–2.00 (m, 2H), 1.27 (m, 80H), 0.92–0.88 (t, 12H); ^{13}C NMR (500 MHz, $CDCl_3$, δ): 163.81, 163.65, 141.79, 131.00, 130.38, 127.92, 126.71, 48.08, 39.10, 34.56, 34.55, 34.18, 32.66, 32.33, 32.31, 32.30, 32.28, 32.26, 32.23, 32.00, 31.98, 28.97, 25.34, 25.33, 16.76; IR (KBr, cm^{-1}): ν = 3048, 2926, 2846, 1710, 1655.

*Synthesis of (E)-1,2-di(thiophen-2-yl)ethene (**3**)*: $TiCl_4$ (6.5 mL) was added drop wise to a slurred solution of 2-thiophenecarbaldehyde (5.6 g, 50 mmol) in THF (100 mL) with stirring, over a period of 30 min at –18 °C. After further stirring at this temperature for 30 min, Zn powder (7.8 g) was added in small portions over a period of 30 min. The mixture was stirred at –18 °C for 30 min, warmed to room temperature, and then refluxed for 3.5 h. The reaction was quenched by adding ice cold H_2O (100 mL) and the resulting solid was collected by filtration and dried. The solid was subsequently dissolved in methylene chloride (80 mL) and the insoluble inorganic material was removed by filtration. The filtrate was evaporated and the residue was recrystallized from hexane to give a yellow product. Yield: 98% (4.70 g) of pure E isomer. ^{1}H NMR (300 MHz, $CDCl_3$, δ): 7.18 (d, 2H), 7.05 (s, 2H), 7.04 (d, 2H), 6.99 (m, 2H).

*Synthesis of (E)-1,2-bis(5-(trimethylstannyl)thiophen-2-yl)ethene (**4**)*: To a solution of (*E*)-1,2-di(thiophen-2-yl)ethene (**3**) (1.78 g, 9.26 mmol) in THF/hexane (2:1, 50 mL), *N*,*N*,*N*′,*N*′-tetramethylethylenediamine (TMEDA, 3.10 mL, 20.7 mmol) was added at –50 °C, and then a 2.0 M solution of *n*-butyllithium in cyclohexane (11 mL, 22 mmol) was drop wise added at –78 °C. The mixture was then refluxed for 1 h. The reaction solution was cooled to –78 °C and a 1.0-M solution of trimethyltin chloride in THF (22 mL, 22 mmol) was added. The solution was warmed to room temperature, stirred for 2 h, and then extracted with diethyl ether. After the removal of the solvent, recrystallization from ethanol afforded the product as pale grey crystals. Yield: 80% (3.88 g). ^{1}H NMR (300 MHz, $CDCl_3$, δ): 7.11 (d, 2H), 7.08 (s, 2H), 7.07 (d, 2H), 0.36 (s, 18H); ^{13}C NMR (500 MHz, $CDCl_3$, δ): 248.23, 237.52, 135.75, 127.00, 121.21, –8.29.

Synthesis of PNDI-TVT: The polymer was prepared using a Pd-catalyzed Stille coupling reaction. NDI-Br_2 (**2**) (0.50 g, 0.46 mmol) and **4** (0.24 g, 0.46 mmol) were dissolved in dry chlorobenzene (7.5 mL). After degassing with N_2 for 1 h, $Pd_2(dba)_3$ (8 mg) and P(*o*-Tol)$_3$ (11 mg) were added to the mixture and stirred for 48 h at 110 °C. Subsequently, 2-bromothiophene and tributyl(thiophen-2-yl)stannane were injected to the reaction mixture for end-capping, and the reaction was stirred for 6 h. The polymer was precipitated in methanol, collected by filtration, and then purified by successive Soxhlet extraction with methanol, acetone, hexane, toluene, and chloroform. The final PNDI-TVT product was obtained by precipitation in methanol. Yield: 91% (0.49 g). M_n = 70 000, M_w = 139 000, PDI = 1.98). ^{1}H NMR (500 MHz, $CDCl_3$, δ): 8.48–8.45 (broad, 2H), 7.93–7.20 (broad, 6H), 4.09–4.08 (broad, 4H), 1.98–1.94 (m, 2H), 1.27–1.24 (m, 80H), 0.87 (m, 12H).

FET Fabrication and Characterization: The Au/Ni (13 nm/2 nm thick) patterns used for the source and drain electrodes were fabricated using a conventional photolithography procedure on Corning Eagle 2000 glass substrates. Substrates were first sequentially cleaned in an ultrasonic bath with deionized water, acetone, and isopropanol for 10 min each, and then baked at 120 °C for 30 min. Before coating with polymer solutions, the Au source and drain electrodes of a proportion of the devices were treated with Cs_2CO_3 as an electron-injection layer. Cs_2CO_3 was dissolved to a concentration of 2 mg mL^{-1} in 2-ethoxyethanol and spin-coated under N_2 onto a patterned glass substrate with Au bottom-contact electrodes at 5000 rpm for 60 s. The substrates were thermally annealed at 120 °C for 30 min in a N_2-filled glove box. PNDI-TVT was dissolved in anhydrous chlorobenzene at a concentration of 10 mg mL^{-1}. The solution was filtered with a 0.2-μm polytetrafluoroethylene syringe filter and spin-coated at 2000 rpm for 60 s in a N_2-filled glove box. The resulting PNDI-TVT films were thermally annealed at various temperatures from room temperature to 210 °C for 10 min under N_2. Poly(methyl methacrylate) (PMMA) (M_w = 120 kD) was used as the dielectric material without further purification. PMMA (80 mg mL^{-1}) was dissolved in *n*-butylacetate and the solution was spin-coated at 2000 rpm for 60 s onto the semiconducting polymer film. The devices were then baked at 80 °C for 2 h under N_2 to remove residual solvent. The transistors were completed by depositing the top-gate electrodes (Al) via thermal evaporation using a metal-shadow mask. The FET electrical characteristics were measured using HP 4156A in a N_2-filled glove box. The μ_{FET} and V_{Th} values were calculated at the saturation region using gradual channel approximation equation.[1]

Supporting Information

Supporting Information is available from the Wiley Online Library or from the author.

Acknowledgements

R.K. and P.S.K.A. contributed equally to this work. This research was financially supported by the National Research Foundation of Korea (NRF) funded by the Ministry of Education, Science and Technology (2012047047 and 2012049647) and by a grant (2012055225 & 2011-0031639) from the Center for Advanced Soft Electronics under the Global Frontier Research Program of the MEST and was supported by the Dongguk University Research Fund of 2013.

Received: April 9, 2013
Published online: June 17, 2013

[1] *Organic Field-Effect Transistors* (Eds: Z. Bao, J. Locklin), Taylor and Francis, Boca Raton, FL **2007**.
[2] H. Klauk, *Chem. Soc. Rev.* **2010**, *39*, 2643.
[3] A. C. Arias, J. D. MacKenzie, I. McCulloch, J. Rivnay, A. Salleo, *Chem. Rev.* **2010**, *110*, 3.
[4] M. Caironi, M. Bird, D. Fazzi, Z. Chen, R. Di Pietro, C. Newman, A. Facchetti, H. Sirringhaus, *Adv. Funct. Mater.* **2011**, *21*, 3371.
[5] H. Zhong, J. Smith, S. Rossbauer, A. J. P. White, T. D. Anthopoulos, M. Heeney, *Adv. Mater.* **2012**, *24*, 3205.
[6] W. Hong, B. Sun, H. Aziz, W.-T. Park, Y.-Y. Noh, Y. Li, *Chem. Commun.* **2012**, *48*, 8413.
[7] J. Liu, D. Haynes, C. Balliet, R. Zhang, T. Kowalewski, R. D. McCullough, *Adv. Funct. Mater*. **2012**, *22*, 1024.
[8] S. G. Hahm, Y. Rho, J. Jung, S. H. Kim, T. Sajoto, F. S. Kim, S. Barlow, C. E. Park, S. A. Jenekhe, S. R. Marder, M. Ree, *Adv. Funct. Mater.* **2013**, *23*, 2060.
[9] K.-J. Baeg, D. Khim, D.-Y. Kim, S.-W. Jung, J. B. Koo, I.-K. You, H. Yan, A. Facchetti, Y.-Y. Noh, *J. Polym. Sci., Part B: Polym. Phys.* **2011**, *49*, 62.
[10] H. T. Nicholai, M. Kuik, G. A. H. Wetzelaer, B. De Boer, C. Campbell, C. Risko, J. L. Brédas, P. W. M. Blom, *Nat. Mater.* **2012**, *11*, 882.
[11] Y. Wen, Y. Liu, *Adv. Mater.* **2010**, *22*, 1331.
[12] X. Zhan, A. Facchetti, S. Barlow, T. J. Marks, M. A. Ratner, M. R. Wasielewski, S. R. Marder, *Adv. Mater.* **2011**, *23*, 268.
[13] F. Würthner, M. Stolte, *Chem. Commun.* **2011**, *47*, 5109.
[14] B. J. Jung, N. J. Tremblay, M.-L. Yeh, H. E. Katz, *Chem. Mater.* **2011**, *23*, 568.
[15] S.-L. Suraru, U. Zschieschang, H. Klauk, F. Würthner, *Chem. Commun.* **2011**, *47*, 11504.
[16] B. Crone, A. Dodabalapur, Y.-Y. Lin, R. W. Filas, Z. Bao, A. LaDuca, R. Sarpeshkar, H. E. Katz, W. Li, *Nature* **2000**, *403*, 521.
[17] H. Yan, Z. Chen, Y. Zheng, C. Newman, J. R. Quinn, F. Dötz, M. Kastler, A. Facchetti, *Nature* **2009**, *457*, 679.
[18] R. Di Pietro, H. Sirringhaus, *Adv. Mater.* **2012**, *24*, 3367.
[19] I. Kang, T. K. An, J.-A. Hong, H.-J. Yun, R. Kim, D. S. Chung, C. E. Park, Y.-H. Kim, S.-K. Kwon, *Adv. Mater.* **2013**, *25*, 524.
[20] D. S. Chung, S. J. Lee, J. W. Park, D. B. Choi, D. H. Lee, J. W. Park, S. C. Shin, Y.-H. Kim, S.-K. Kwon, C. E. Park, *Chem. Mater.* **2008**, *20*, 3450.
[21] J. H. Kwon, J.-Y. An, H. Jang, S. Choi, D. S. Chung, M.-J. Lee, H.-J. Cha, J.-H. Park, C. E. Park, Y.-H. Kim. *J. Polym. Sci., Part A: Polym. Chem.* **2011**, *49*, 1119.
[22] B. A. Jones, A. Facchetti, M. R. Wasielewski, T. J. Marks, *J. Am. Chem. Soc.* **2007**, *129*, 15259.
[23] S. Fabiano, C. Musumeci. Z. Chen, A. Scandurra, H. Wang, Y.-L. Loo, A. Facchetti, B. Pignataro, *Adv. Mater.* **2012**, *24*, 951.
[24] H. Pan, Y. Li, Y. Wu, P. Liu, B. S. Ong, S. Zhu, G. Xu, *J. Am. Chem. Soc.* **2007**, *129*, 4112.
[25] H.-S. Kim, Y.-H. Kim, T.-H. Kim, Y.-Y. Noh, S. Pyo, M. H. Yi, D.-Y. Kim, S.-K. Kwon, *Chem. Mater.* **2007**, *19*, 3561.
[26] Y.-Y. Noh, X. Cheng, M. Tello, M.-J. Lee, H. Sirringhaus, *Semicond. Sci. Technol.* **2011**, *26*, 034003.
[27] a) K.-J. Baeg, J. Kim, D. Khim, M. Caironi, D.-Y. Kim, I.-K. You, J. R. Quinn, A. Facchetti, Y.-Y. Noh, *ACS Appl. Mater. Interfaces* **2011**, *3*, 3205; b) D. Khim, K.-J. Baeg, J. Kim, J.-S. Yeo, M. Kang, P. S. K. Amegadzea, M.-G. Kim, J. Cho, J. H. Lee, D.-Y. Kim, Y.-Y. Noh, *J. Mater. Chem.* **2012**, *22*, 16979.